Energy levels of Tm^{3+} in yttrium aluminium garnet

Energy levels of Tm^{3+} in yttrium aluminium garnet

C Tiseanu, A Lupei and V Lupei

Institute of Atomic Physics, Bucharest 76900, Romania

Abstract. An improved energy level diagram for Tm^{3+}(4f^{12}) ions in dodecahedral (D$_2$ symmetry) sites in Y$_3$Al$_5$O$_{12}$ (YAG) has been obtained from experimental absorption and emission spectra. Interferences in line assignment from the spectra of minority perturbed Tm^{3+} centres or due to electron–phonon interaction are discussed. A parametrized Hamiltonian that includes one-electron crystal-field interactions for D$_2$ symmetry has been used to fit the experimental data. The RMS deviation between 70 experimentally determined levels (from the total of 90) and calculated levels is 9 cm^{-1} and the individual misfit is no larger than 20 cm^{-1}. The analysis is based not only on the experimentally located energy levels, but also on the information concerning the symmetry labels for Stark levels. The obtained set of crystal-field parameters seems more suitable than the previously reported description of Tm^{3+} crystal-field energy levels in YAG.

1. Introduction

In the 2 μm laser emission, Tm^{3+}(4f^{12}) plays an important role either as emitting ion or as sensitizer for Ho^{3+}. Co doping with transition-metal ions such as Cr^{3+} increases the laser efficiency in both cases. As host crystals the most appropriate seem to be the garnets, not only because of their thermal or mechanical properties and their known growth technology, but also owing to the spectral characteristics of Tm^{3+}. The ^{3}F$_4$ → ^{3}H$_6$ emission cross sections and the ground multiplet (^{3}H$_6$) splitting are rather large (about 800 cm^{-1} in Y$_3$Al$_5$O$_{12}$ (YAG)) and thus the population of the lower laser level is negligible, assuring a four-level laser system operation. Taking into account these characteristics, YAG is one of the most convenient host laser crystals for doping with Tm^{3+}. However, the spectral characteristics of YAG: Tm^{3+} are still incompletely known. A schematic energy level diagram of Tm^{3+} in YAG is presented later in figure 5. The detailed energy level diagrams including the assignment of symmetry labels for Stark levels previously proposed for Tm^{3+} in YAG [1, 2] show noticeable differences, some of them in the multiplets involved in the 2 μm laser emission.

Tm^{3+} ions enter preponderantly in dodecahedral garnet c sites of local D$_2$ symmetry and all the Stark levels are singlets that could be characterized by one of the four irreducible representations Γ_i ($i = 1$–4). Several difficulties connected with the problem of determining the energy level diagram should be mentioned.

(i) The Γ_i → Γ_i transitions are electric and magnetic dipole forbidden in D$_2$. Thus, in the low-temperature absorption spectra, some of the lines are missing; by using a hot band structure (temperature-activated transitions) and luminescence spectra this difficulty could

be sometimes overcome. Large differences between the line intensities have also been observed; some of low-intensity lines of the main centre are comparable with high-intensity lines connected with other minority centres.

(ii) There is a complex multisite structure of Tm^{3+} in garnets due to non-equivalent perturbed centres. The nature of these centres is not completely known; the main satellite lines could be assigned to three types of centres: perturbed centres due to garnet non-stoichiometric defects [2,3], Tm^{3+}–Tm^{3+} pairs or Tm^{3+} in octahedral a sites. The spectra connected with these centres are more complex, and the lines are rather sharp; the local symmetry is generally lower than D_2 and $\Gamma_i \rightarrow \Gamma_i$ restriction is no longer valid. The multisite structure together with hot bands has been previously [2] used to assign some of the Stark leels for which the transitions in D_2 are forbidden.

(iii) Phonon interferences occur. The most known phonon effect is the broadening of spectral lines corresponding to transitions to higher Stark levels of the same multiplet. Another effect observed for some Tm^{3+} transitions in YAG is a complex structure with broad lines, suggesting a vibronic nature of the transitions. We shall present the spectra connnected with transitions to $^3H_6$ and $^3H_4$ multiplets and a very peculiar behaviour observed in absorption to the $^3F_2$ multiplet that could present phonon interferences. This structure creates problems in the experimental separation of 'pure' electronic transitions from the phonon-assisted transitions. A similar behaviour has been signalled for Pr^{3+} ($4f^2$) spectra in garnets. In the case of Pr^{3+} in YAG it was suggested [4] that an electron–phonon interaction occurs through resonance with peaks in the density of phonon states and the ground-state ($^3H_4$) Stark levels, that have energies in the 350–750 cm^{-1} range. The density of the phonon spectrum of the YAG lattice is large in this spectral range. For rare earths in solids the possibility of small energy shifts of some Stark levels due to the interaction with high density of phonons, especially for lower-lying levels in a configuration was tentatively proposed [5].

The assignment of symmetry labels could be experimentally made either by selective polarized excitation and emission spectra, based on the technique developed in [6] for isotropic cubic garnet crystals, or by using non-polarized spectra and an algorithm presented in detail in [1] and with an improvement in [2]. The algorithm predicts, by lattice sum calculation, the symmetry of the ground Stark level (Γ_2 for Tm^{3+} in YAG) and then, by using the positions of hot bands in absorption and laser-excited luminescence lines from specific Stark levels, symmetry labels could be assigned to other Stark levels. The results of the symmetry assignment for the most intense lines are finally compared with those of a parametrized crystal-field calculation. Due to our experimental possibilities as well as to the difficulties in obtaining reliable polarization data (several dye lasers, depolarization due to interferences with low-symmetry centres, samples quality, etc) we have chosen the second technique with good results in the analysis of Tm^{3+} energy levels in GGG [7].

The purpose of this paper is an attempt to improve the energy level diagram for the main Tm^{3+} centre in YAG based on absorption, luminescence and excitation unpolarized spectra and to obtain a set of crystal-field parameters that describes the data accurately. Our previous energy level scheme, obtained from experimental data (some of them performed only at temperatures greater than 77 K), was limited to lower multiplets (up to $^3F_2$) involved effectively in 2 μm laser emission. We have extended the data by absorption to higher multiplets and analysed the possible interferences in order to improve the experimental data. A parametric crystal-field calculation has been performed using these improved data. A comparison between the crystal-field parameters obtained in this investigation and the previously reported values is also presented.

2. Experiment

Single crystals of YAG: Tm^{3+} (0.1–5 at.%) Czochralski-grown have been spectrally investigated, at various temperatures between 4 and 300 K. The IR and UV spectra have been measured with a Cary 17 spectrometer and part of a visible spectrum with an experimental set-up for transmission [2]. The emission was excited with the third harmonic of a YAG: Nd Quanta-Ray laser, dispersed with a 1 m GDM monochromator and detected with an S20 photomultiplier and a boxcar integrator. A dye laser has been used for selective excitation.

3. Results

3.1. Experimental data

The absorption and emission spectra under 355 nm excitation of the $^1D_2$ level, at different temperatures, enabled us to obtain experimental values of the Tm^{3+} Stark levels for all the multiplets except $^1S_0$ (table 1). For multiplets higher than $^1G_4$, data were obtained only from absorption spectra and some of the levels have been assigned only from the hot band structure. Symmetry labels have been assigned to several Stark levels (table 1) by the algorithm used earlier [1, 2] and some of the ambiguities have been eliminated by iterative comparison with crystal-field calculations. Several important differences between the data given in table 1 and those previously reported [1] have been observed; those regarding the low multiplets (up to $^1G_4$) have been discussed in our previous report [2]. We shall point out only the main experimental problems that might lead to these differences and our approach to solve them.
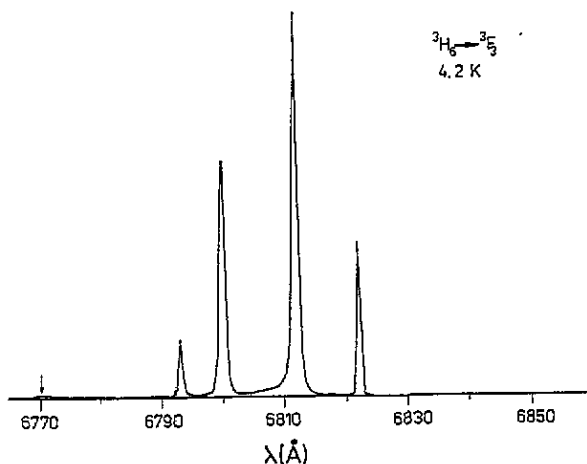

Figure 1. Excitation spectrum (at 4.2 K) of the $^3H_4 \rightarrow {}^3H_6$ emission in the region of $^3H_6 \rightarrow {}^3F_3$ absorption.

As mentioned above, it is difficult to determine whether some lines are due to weak transitions in D_2 or to strong transitions connected with minority centres. Some ambiguities have been solved for the $^3F_3$ multiplet (that presents the most intense lines in the spectra and a very rich satellite structure) by using laser-selective excitation spectra at low temperatures. Thus, in figure 1 the excitation spectrum for $^3F_3$ (at 4.2 K) of the $^3H_4$ main centre emission (by monitoring the 12363 cm^{-1} emission line corresponding to the $^3H_4(1) \rightarrow {}^3H_6(3)$

Table 1. Energy levels of Tm^{3+} ions in D_2 sites; (c), calculated centroid for $^{2S+1}L_J$; Γ_n, irreducible representations.

$^{2S+1}L_J$	Experiment		Calculation	
	E (cm^{-1})	Γ_n	E (cm^{-1})	Γ_n
$^3H_6$	0	2	−10	2
(451) (c)	27	1	12	1
	216	4	235	4
	240	3	237	3
	247	2	250	2
	300		304	1
	450		461	4
	588		589	1
	610		614	3
	650		647	2
	690		688	4
	730[a]		781	3
	—		798	1
$^3F_4$	5555	1	5545	1
(5982) (c)	5764	3	5763	3
	5832	2	5827	2
	5901	4	5906	4
	6042	1	6048	1
	6111	2	6119	2
	6170	1	6175	1
	—		6175	3
	6199	4	6190	4
$^3H_5$	8340	4	8345	4
(8629) (c)	8345	3	8347	3
	8516	1	8510	1
	8530	3	8525	3
	8556	2	8552	2
	—		8577	4
	8700	2	8687	2
	8750		8761	3
	8773		8766	1
	—		8900	2
	—		8901	4
$^3H_4$	12607	1	12591	1
(12 889) (c)	12644	2	12652	2
	12732	2	12733	2
	12747	4	12751	4
	12824	3	12833	3
	—		12973	1
	13036	4	13038	4
	13112		13113	1
	13152		13149	3
$^3F_3$	14599	2	14613	2
(14 662) (c)	14659	4	14658	4
	14666	2	14663	2
	14679	4	14687	4
	14706	3	14690	3
	14720	1	14716	1
	14770[a]	3	14748	3

Table 1. (Continued)

$^{2S+1}L_J$	Experiment		Calculation	
	E (cm^{-1})	Γ_n	E (cm^{-1})	Γ_n
$^3F_2$	15 190	3	15 202	3
(15 260) (c)	15 246	1	15 245	1
	15 263	4	15 252	4
	—		15 397	2
	—		15 408	1
$^1G_4$	20 806	1	20 818	1
(21 461) (c)	21 212	2	21 199	2
	21 228	3	21 230	3
	21 381	4	21 373	4
	21 530	1	21 516	1
	21 680	2	21 680	2
	21 735	4	21 748	4
	21 775	3	21 764	3
	—		21 764	1
$^1D_2$	27 868	1	27 876	1
(27 974) (c)	27 877	3	27 896	3
	28 016	2	28 010	2
	28 042	4	28 034	4
	28 070	1	28 061	1
$^1I_6$	34 370		34 363	1
(34 816) (c)	—		34 373	4
	34 420		34 418	3
	—		34 464	4
	34 520		34 524	4
	—		34 717	3
	34 746		34 735	1
	—		34 938	1
	—		34 939	2
	—		35 220	2
	—		35 226	2
$^3P_0$	35 372	1	35 372	1
(35 372) (c)				
$^1I_6$	35 388		35 385	3
$^3P_1$	—		35 402	1
(36 337) (c)	36 231		36 229	3
	36 390		36 395	4
			36 419	2
$^3P_2$	37 933		37 943	3
(38 159) (c)	38 065		38 063	4
	38 097		38 090	1
	38 400		38 408	1
	—		38 430	2

[a] Levels not included in the final fitting procedure.

transition) is presented. Four of the five allowed $^3H_6(\Gamma_2) \rightarrow {}^3F_3(\Gamma_1, 2\Gamma_3, 2\Gamma_4)$ transitions are clearly observed; one has to mention, however, the low intensity of one of the lines

(indicated by an arrow) that we have assigned to an allowed transition in D_2. This assignment was sustained by $^1D_2$ emission (see figure 9 of [2]). This rather simple spectrum has to be compared with the absorption (see figure 4 later) where a multitude of lines due to minority centres are observed in the $^3H_6 \rightarrow ^3F_3$ spectral range.

The experimental energy level scheme is slightly different from our previous proposal [2] too. The main problems appear in the $^3H_6$, $^3H_4$ and $^3F_2$ multiplets and seem to be connected with phonon interferences. The Stark levels of the $^3H_6$ multiplet are obtained from the $^1D_2$, $^1G_4$ and $^3H_4$ emission spectra at low temperatures (or hot band structure). For all these excited multiplets (including $^3F_4$), the ground Stark level has Γ_1 symmetry and therefore $^3H_6$ levels with the same symmetry label (Γ_1) are difficult to localize from emission at low temperatures. In the case of $^1D_2$ and $^3H_4$ multiplets, the emission from the second Stark level (Γ_3 and Γ_2, respectively) is also observed at 77 K and this way some of the Γ_1 Stark levels of the $^3H_6$ multiplet have been assigned. In figure 2 the $^1G_4 \rightarrow ^3H_6$ emission spectrum at 77 K under excitation of $^1D_2$ is presented. If the lines corresponding to transitions to the $^3H_6$ levels situated up to about 250 cm^{-1} are rather intense and sharp, in the 300–800 cm^{-1} range more lines than allowed by the selection rules are observed and they are broad; most probably transitions to electronic Stark levels are overlapping with phonon-assisted transitions. In the $^3H_6(\Gamma_2) \rightarrow ^3H_4$ absorption at 4.2 K (figure 3), instead of seven lines allowed by symmetry a much more complex spectrum is also observed, especially in the 12 900–13 200 cm^{-1} range. The shape of the line at 13 075 cm^{-1} suggests that this is possibly a phonon side band, the phonon spectrum having a strong peak at 465 cm^{-1}. The levels given in table 1 have been assigned by an iterative multistep comparison with the crystal-field calculation.
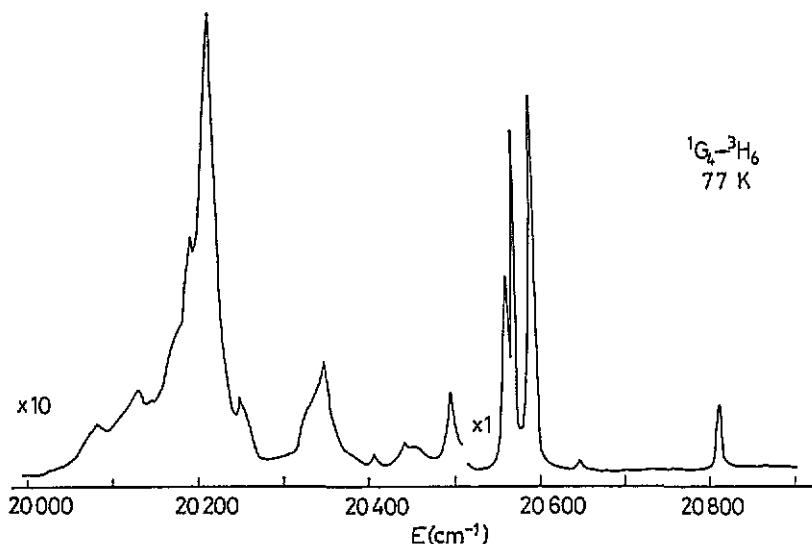

Figure 2. The $^3G_4 \rightarrow ^3H_6$ emission at 77 K on excitation with 355 nm.

A special situation is observed in the $^3H_6 \rightarrow ^3F_2$ absorption spectra (figure 4) where the spectrum at 77 K reveals some of the hot bands too. Our previous assignment included two Stark levels at 15 183 and 15 190 cm^{-1}, while in [1] the first Stark level of $^3F_2$ was identified at 15 246 cm^{-1}. Our assignment was based on the absorption intensities, on the lack of other intense phonon side bands connected with the $^3F_3$ multiplet, on the presence
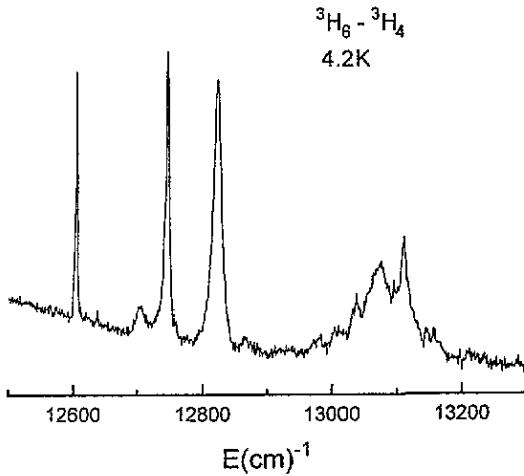
Figure 3. Transmission spectrum corresponding to the $^3H_6 \rightarrow {}^3H_4$ transition at 4.2 K.
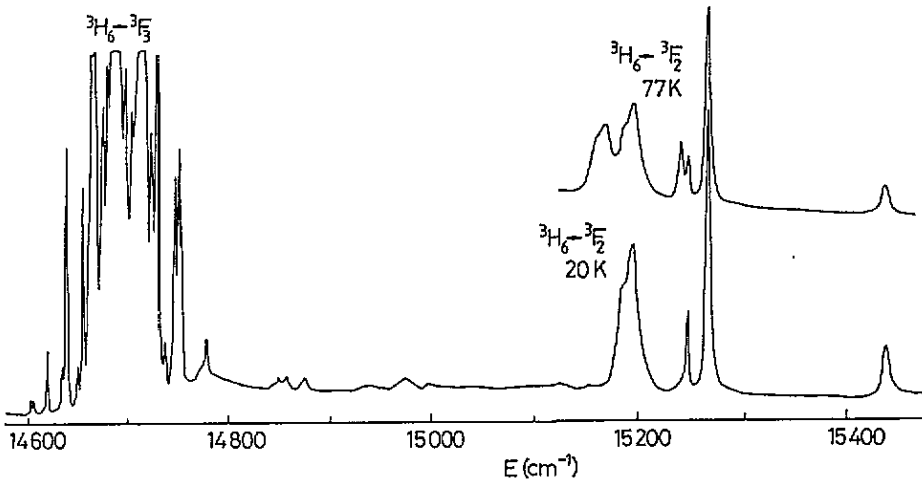

Figure 4. Transmission spectra corresponding to the $^3H_6 \rightarrow {}^3F_3$, $^3F_2$ transitions at 20 and 77 K.

of hot bands at 27 cm^{-1} for both lines (figure 4) and on the comparison with the splitting of this multiplet in other garnets. An argument against our assumption could be that these lines are rather broad compared with lines at higher energies.

4. Crystal-field calculation

The experimentally determined Stark levels of Tm^{3+} in YAG, given in table 1, together with the free-ion Russell–Saunders [SLJ] states of the free-ion Hamiltonian containing the Coulomb, spin–orbit, L^2, $G(G_2)$ and $G(R_7)$ interactions [8] have been used in a parametrized crystal-field calculation.

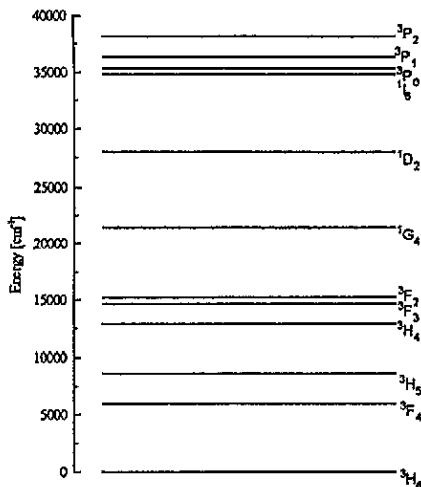The crystal-field Hamiltonian H_{CF} used in the calculation represents the anisotropic

Figure 5. Schematic energy level diagram of Tm^{3+} in YAG.

components of the one-electron crystal-field interactions:

$$H_{CF} = \sum_{k,m} B_{km}^* \sum_i C_{km}(\hat{r}_i) \tag{1}$$

where the B_{km} parameters contain the radially dependent parts of the one-electron crystal-field interactions, and $C_{km}(\hat{r}_i)$ are single 4f operators related to the spherical harmonic operators Y_{km} by

$$C_{km}(\hat{r}_i) = [4\pi/(2k+1)]^{1/2} Y_{km}. \tag{2}$$

The values taken by k are limited to 2, 4 and 6 as all matrix elements of the crystal-field Hamiltonian are taken between states of a single configuration; for the D_2 symmetry the permitted values of m are 0, ± 2, ± 4, ± 6 and the sum on i in equation (1) covers the 12 electrons of the $4f^{12}$ configuration. Since the positions of the experimental energy levels of Tm^{3+}: YAG and Tm^{3+}: YSAG [9] are quite similar, we have chosen, as starting parameters in the least-squares fitting, the crystal-field parameters obtained for Tm^{3+} in YSAG [9]. This set of parameters gave good results from the first iterative steps, unlike other sets of parameters reported for Tm^{3+} in garnets [1, 7]. The phenomenological crystal-field parameters have been obtained by a least-squares fit of the calculated energy levels to some of the experimental energy levels. The fitting of calculated versus experimental data has been performed by treating the nine parameters B_{km} as free variables, permitting also the centroids of the $[SL]J$ multiplets to vary freely. Interferences between atomic and crystal-field parameters are avoided this way; the crystal-field parameters become entirely free together with multiplet baricentres. However, since the $[SL]J$ basis functions used in these calculations are derived from an approximate atomic Hamiltonian, the inaccuracies in these functions could distort the crystal-field parametrization results. The resulting parameters (in reciprocal centimetres) obtained in our calculation that give the best fit are given in table 2, while the calculated Stark levels and the corresponding irreducible representations are presented in table 1. For comparison the crystal-field parameters reported for Tm^{3+} in YAG [1] and YSAG [9] are also given in table 2.

Table 2. Comparison between crystal-field parameters in YAG and YSAG and their corresponding rotational invariants.

Garnet	B_{20} (cm⁻¹)	B_{22} (cm⁻¹)	B_{40} (cm⁻¹)	B_{42} (cm⁻¹)	B_{44} (cm⁻¹)	B_{60} (cm⁻¹)	B_{62} (cm⁻¹)	B_{64} (cm⁻¹)	B_{66} (cm⁻¹)	S_2 (cm⁻¹)	S_4 (cm⁻¹)	S_6 (cm⁻¹)
YAG [1]	474	47	−213	−1571	−824	−984	−310	591	−193	476	1786	1204
YSAG [8]	667	54.1	−22.5	−1502	−702	−835	−465	566	−272	669	1658	1143
YAG (this work)	603	39	−59	−1441	−707	−1181	−302	448	−360	604	1606	1348

5. Discussion

The set of crystal-field parameters obtained in this work and that previously reported [1] are different (table 2), the reason being the experimental assignment of Stark levels connected with the main Tm³⁺ centre. The RMS deviation between 70 experimentally determined levels (from the total of 90) and calculated levels is 9 cm⁻¹ and the individual misfit is no larger than 20 cm⁻¹; this represents an improvement of fit compared with [1]; an example is $^1D_2$ for which our set of crystal-field parameters underestimate the global splitting by about 15 cm⁻¹ compared with about 50 cm⁻¹ given by the set in [1], even if the experimental Stark levels and irreducible representations are similar. Except for $^1S_0$ situated at around 79 600 cm⁻¹ (table 1), we did not leave out any other multiplets from the final fitting. We have also studied the variation in the crystal-field parameters if some multiplets are excluded from fitting. They are relatively insensitive (to within ±5–10%) to the exclusion of the $^3F_4$, $^1G_4$, $^1D_2$ and $^3P_2$ multiplets, but more sensitive (±10%) to the exclusion of the $^3H_5$, $^3H_4$, $^3F_3$ and $^3F_2$ multiplets. A significant variation in B_{20} (decreases by about 25%) and B_{40} (increases by about 200%) has been observed if the ground-state multiplet $^3H_6$ is excluded from the fit; this influences especially the position and symmetry labels for the $^3H_5$ and $^3H_4$ Stark components. The inaccuracies in experimental data for some multiplets are large so that the inclusion of certain additional correlation operators in the model Hamiltonian seems at this point meaningless.

   In order to compare the RMS error obtained for crystal fields of different strengths, Leavitt [10] has proposed the concept of rotational invariance, the rotational invariants S_k being defined as

$$S_k = \left[\sum_{m=-k}^{k} B_{km}^* B_{km} \right]^{1/2} \tag{3}$$

for $k = 2$, 4 and 6. The comparison between the values of S_k for Tm³⁺: YSAG and those estimated for Tm³⁺: YAG (table 2) shows that these values are quite similar for our set of crystal-field parameters, in accord with the similarity of experimental levels. The difference between cell sizes of YAG ($a = 12$ Å) and YSAG ($a = 12.271$ Å) would suggest greater values for the crystal-field parameters in YAG than in YSAG; however, the rotational invariants are comparable since the crystal-field parameters are predominantly determined by the nearest-neighbour oxygen ions. Indeed, the nearest oxygen ions are situated at 2.303 Å (×4) and 2.432 Å (×4) from the yttrium site in YAG and at 2.338 Å (×4) and 2.440 Å (×4) in YSAG [8]. Similar values of the ten crystal-field parameters for Nd³⁺ [11] and Er³⁺ [12] in YAG and YSAG have been reported.

   The parametrized crystal-field calculation has been used to separate the Stark levels from phonon-assisted transitions. Since the number of experimental energy levels clearly assigned is much larger than that of the crystal-field parameters, we have been able to

assign, by an iterative procedure, some of the Stark levels of $^3H_6$, $^3H_4$ and $^3F_2$ multiplets where phonon interferences were observed (table 1).

For rare-earth ions in crystals, two types of vibronic line are generally discussed: Δ-type transitions that correspond to Franck–Condon replicas and M-type that are vibronically forced electric-dipole transitions, resulting from the diagonal and off-diagonal parts, respectively, of the Hamiltonian of electron–phonon coupling [13, 14]. Since for the main Tm^{3+} centre the local symmetry is low (D_2) and $\Gamma_i \rightarrow \Gamma_i$ transitions are forbidden, both types of vibronic line, i.e. Δ or M, are possible. The possibility of small energy shifts of some Stark levels owing to resonant interaction with phonons has also been considered [5]. In the ground-state $^3H_6$ and the excited-state $^3H_4$ multiplet, the most intense phonon interferences appear in regions where the resonances between the difference in electronic energies inside a given multiplet and the high-density phonon spectrum are possible. Taking into account the results of the crystal-field calculation, only one Stark level of $^3F_2$ could be situated around 15 190 cm^{-1}; the absorption spectrum in figure 4 could thus be explained by an overlap with a phonon side band connected with the $^3F_3$ multiplet. However, other phonon side bands connected with this multiplet have rather small intensities as can be observed in figure 4. The problem of phonon interferences needs further consideration, since perturbed centres of lower symmetry could also play a role as suggested for Pr^{3+} in YAG [15].

In conclusion, we have analysed the experimental data that span 13 (from the total of 14) $^{2S+1}L_J$ multiplets of Tm^{3+} in YAG. Our attention has focused on the location of the crystal-field levels assigned to Tm^{3+} substituted in Y^{3+} dodecahedral c sites (D_2 symmetry) and using an algorithm [1, 2] the symmetry labels have been identified for about 50 Stark levels. A parametrized Hamiltonian that includes one-electron crystal-field interactions has been used to fit the experimental Stark levels. A multistep crystal-field calculation has allowed us to obtain a rather accurate energy level scheme for Tm^{3+} in YAG.

References

[1] Gruber J B, Hills M E, Macfarlane R M, Morrison C A, Turner G A, Quarless G J, Kintz G J and Esterowits L 1989 *Phys. Rev.* B **40** 9464
[2] Lupei A, Tiseanu C and Lupei V 1993 *Phys. Rev.* B **47** 14 084
[3] Lupei V, Lupei A and Boulon G 1994 *J. Physique IV* **4** 407
[4] Antic-Fidancev E, Lemaitre-Blaise M and Krupa J C 1988 *Czech. J. Phys.* B **38** 1268
[5] Caro P 1986 *J. Less Common Met.* **126** 239
[6] Bayerer R, Heber J and Mateika D 1986 *Z. Phys.* B **64** 201
[7] Lupei A, Lupei V, Grecu S and Tiseanu C 1994 *J. Appl. Phys.* **75** 4652
[8] Carnall W, Fields P and Rajnak K 1968 *J. Chem. Phys.* **49** 4412
[9] Gruber J, Seltzer M, Hills M, Stevens S and Morrison C 1993 *J. Appl. Phys.* **73** 1929
[10] Leavitt R P 1982 *J. Chem. Phys.* **73** 1661
[11] Allik H T, Morrison C A, Gruber J B and Kokta M R 1990 *Phys. Rev.* B **41** 21
[12] Gruber J B, Quagliano J R, Reid M F, Richardson F S, Hills M E, Seltzer M D, Stevens S B, Morrison C A and Allik H T 1993 *Phys. Rev.* B **48** 15 561
[13] Myakava 1973 *Luminescence of Crystals, Molecules and Solutions* ed R Williams (New York: Plenum) p 394
[14] Dexpert-Ghys J and Auzel F 1984 *J. Chem. Phys.* **80** 4003
[15] Dennis W M 1993 *Proc. 12th Int. Conf. on Defects in Insulating Materials* vol 1, ed O Kanert and J M Spaeth (Singapore: World Scientific) p 380